Fast algorithm for solving hybrid integral equations

C.C. Lu
W.C. Chew, PhD

Indexing terms: Algorithms, Integral equations, Hybrid equations, Dielectric-coated conducting cylinder, Matrix–vector multiplication

Abstract: A fast algorithm is presented to solve for the scattered field of a two-dimensional, dielectric-coated conducting cylinder using a hybrid of a combined field surface integral equation and volume integral equation. The fast algorithm is an extension of the fast multipole method and it relies on the translation of scattering centers to speed up the matrix–vector multiplication in the conjugate gradient method. The scatterer is first divided into many subscatterers. Instead of directly computing the matrix–vector multiplication, which needs N^2 multiplications, an efficient approach is used to reduce the floating-point operation count required. The algorithm has a computational complexity of $O(N^{1.5})$.

1 Introduction

Computation of the scattering solution by two-dimensional (2D) conducting cylinders is a classical electromagnetic problem, and many algorithms have been developed for this purpose [1–6]. In most cases, the problem is converted into an integral equation where the unknown function is the induced current distribution. The integral equation is then solved by the method of moments (MOM) [7] which requires $O(N^3)$ floating-point operations if Gaussian elimination is used to invert the N by N matrix, or N^2 operations per iteration if the conjugate gradient (CG) method is used [8].

Recently, Rokhlin [9] has developed a fast multipole method for acoustic wave scattering problems. The method has been applied to electromagnetic scattering computation of the E_z-polarised case by Engheta *et al.* [10]. In this paper, we will extend the algorithm to the H_z-polarised case and apply it to calculate the scattering solution of dielectric-coated conducting cylinders. A combined-field surface integral equation [11, 12, 13] will be used to remove the internal resonance problem for the metallic scatterer, and a hybrid combined-field surface integral equation and volume integral equation will be used to solve the problem involving dielectric coating. We shall also present an alternate derivation and physical interpretation of this fast algorithm. As will be obvious from the derivation, the waves are expressed as plane waves as they propagate from one scattering centre to another.

Paper 9667H (E12), first received 20th October 1992 and in revised form 26th March 1993

The authors are with the department of Electrical and Computer Engineering, University of Illinois, Urbana, IL 61801, USA

In this algorithm, a metallic scatterer is first decomposed into N subscatterers [9]. When there is an incident wave, each subscatterer will carry a current distribution which is determined by the interaction equation (the discretised integral equation). To compute the total field at a subscatterer due to the other subscatterer, one needs at least N multiplications. Since there are N subscatterers N^2 multiplications are needed to compute the total interactions among them. These N^2 interactions correspond to a matrix–vector multiplication in a conjugate-gradient method.

The fast multipole method [9] is designed to account for this interaction more efficiently. The idea is first to divide the subscatterers into groups. Then, the addition theorem of Bessel functions (or the translation matrix) is used to translate the scattered field of different scattering centres within a group into a single centre (called group centre). Hence, one scattering centre represents the scattered field of a group of centres, reducing the number of scattering centres. Similarly, for each group, the field scattered by all the other group centres can be first 'received' by the group centre, and then redistributed to the subscatters belonging to the group.

In fact, since each subscatterer is a monopole (for the E_z wave) or a dipole (for the H_z case), the group centre will be a higher-order multipole. Hence, the reduction in the number of scattering centres is at the expense of increasing the order of the multipoles. However, it can be shown that by appropriately selecting the size of the groups and diagonalising the translation matrices with plane-wave basis, the number of floating-point operations needed to compute the overall interaction can be reduced from N^2 to $N^{1.5}$. A further nesting of the algorithm yields an $O(N^{1.33})$ algorithm.

2 New look at the fast multipole method

The fast multiple method [9] is designed to speed up the matrix–vector multiplication in the CG method when CG is used to solve a surface integral equation. We shall present here a more succinct derivation of this algorithm.

As an example, the surface integral equation which governs the scattering solution of a metallic scatterer by E_z-polarised waves is given by

$$i\omega\mu_0 \int_s dS' g_0(\rho - \rho') J_z(\rho') = -E_z^{inc}(\rho) \quad \rho \in S \tag{1}$$

This work was supported by Office of Naval Research under grant N00014-89-J1286, and the Army Research Office under contract DAAL03-91-G-0339. The computer time was provided by the National Center for Supercomputing Applications (NCSA) at the University of Illinois, Urbana-Champaign.

In the above

$$g_0(\rho - \rho') = \frac{i}{4} H_0^{(1)}(k|\rho - \rho'|) \tag{2}$$

$J_z(\rho')$ is the induced current on the surface of the scatterer and $E_z^{inc}(\rho)$ is the incident field. The above integral equation can be discretised [7] to yield

$$\sum_{i=1}^{N} g_{ji} a_i = b_j \quad j = 1, \ldots, N \tag{3}$$

where

$$g_{ji} = \begin{cases} \dfrac{\omega\mu_0}{4}\left[1 + \dfrac{2i}{\pi}\ln\left(\dfrac{\gamma k \Delta_i}{4e}\right)\right] & \Delta i, i = j \\ \dfrac{\omega\mu_0}{4}\Delta_i H_0^{(1)}(\kappa\rho_{ji}) & i \neq j \end{cases} \tag{4a}$$

$$b_j = E_z^{inc}(\rho_j) \tag{4b}$$

$$a_i = J_z(\rho_i) \tag{4c}$$

where $\rho_{ji} = |\rho_j - \rho_i|$ and $(\gamma/4e) = 0.163805$. The matrix–vector multiplication, $\sum_{i=1}^{N} g_{ji} a_i$, is the bottleneck in the speed of the CG algorithm. The fast multipole method expedites this matrix–vector multiplication. This is achieved by dividing the N subscatterers into groups, each of which contains M subscatterers. Hence, there are N/M groups altogether. Furthermore, the translational addition theorem can be used to rewrite g_{ji}. Using the notation developed by us previously [14–18], we can write

$$H_0^{(1)}(k\rho_{ji}) = \overbrace{\boldsymbol{\beta}_{jl'}^t}^{1\times P} \cdot \overbrace{\bar{\boldsymbol{\alpha}}_{l'l}}^{P\times P} \cdot \overbrace{\boldsymbol{\beta}_{li}}^{P\times 1} \tag{5}$$

where l' and l are the centres of the l'th and lth groups, respectively (Fig. 1) and $\bar{\alpha}$ and β are defined in References 15–18. They are given here explicitly as

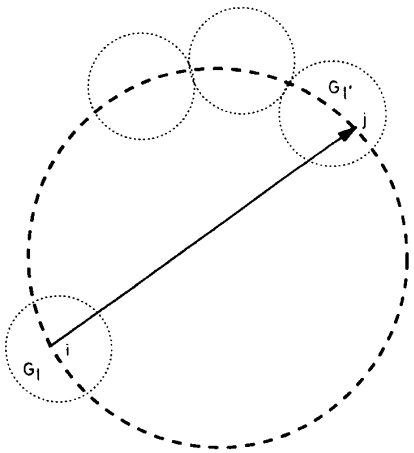

Fig. 1 *For an arbitrarily-shaped surface scatterer (e.g. metallic scatterer), the scatterer is decomposed into N subscatterers. The N subscatterers are divided into groups of size $O(\sqrt{N})$. The interaction between the subscatterers are calculated via their group interactions*

$$[\bar{\alpha}_{l'l}]_{nm} = H_{n-m}^{(1)}(k_0\rho_{l'l})e^{-i(n-m)\phi_{l'l}} \tag{5a}$$

$$[\beta_{jl'}]_n = J_n(k_0\rho_{jl'})e^{-in\phi_{jl'}} \tag{5b}$$

where $\phi_{l'l}$ is the angle the line $\rho_{l'l}$ makes with the x-axis and similarly for $\phi_{jl'}$. Using eqn. 5, we can rewrite eqn. 3 as

$$\frac{\omega\mu_0}{4}\boldsymbol{\beta}_{jl'}^t \sum_{\substack{l=1 \\ l\neq l'}}^{N/M} \bar{\boldsymbol{\alpha}}_{l'l} \sum_{i\in G_l} \boldsymbol{\beta}_{li}\Delta_i a_i = b'_j$$

$$j \in G_{l'} \quad l' = 1, \ldots, N/M \tag{6}$$

for interactions between elements of group G_l and group $G_{l'}$ only. In the above, b'_j is used to indicate interactions excluding the interaction within the same group. For interactions between elements within the same group, eqn. 3 is still used.

To maintain the accuracy of eqn. 5, $P \approx cM$ because the number of cylindrical harmonics P needed in eqn. 5 is proportional to the size of the group, and M is proportional to the size of the group. Hence, the cost of computing $\boldsymbol{c}_l = \sum_{i\in G_l} \boldsymbol{\beta}_{li}\Delta_i a_i$, $l = 1, \ldots, N/M$ is

$$T_1 = c_1 \frac{N}{M} M^2 = c_1 NM \tag{7}$$

The cost of computing $\boldsymbol{d}'_l = \sum_{l=1}^{N/M} \bar{\boldsymbol{\alpha}}_{l'l} \cdot \boldsymbol{c}_l$, $l = 1, \ldots, N/M$ is

$$T_2 = c_2\left(\frac{N}{M}\right)^2 M^2 = c_2 N^2 \tag{8}$$

The cost of computing $\boldsymbol{\beta}_{jl'}^t \cdot \boldsymbol{d}_{l'}$, $j \in G_{l'}$, $l', \ldots, N/M$ is

$$T_3 = c_3\left(\frac{N}{M}\right) M^2 = c_3 NM \tag{9}$$

Therefore, there is little advantage at this point in rewriting eqn. 3 as eqn. 6 as now the cost of performing eqn. 6 still requires $O(N^2)$ operations. However, the cost of calculating eqn. 6 can be substantially reduced if $\bar{\alpha}$ can be diagonalised.

To this end, we substitute in the definition of $\bar{\alpha}$ and $\boldsymbol{\beta}$ [18] in eqn. 5, so that it can be written as

$$H_0^{(1)}(k\rho_{ji}) = \sum_{m=-\infty}^{\infty} J_m(k\rho_{jl'})e^{im(\phi_{jl'}-\pi)} \times \sum_{n=-\infty}^{\infty} H_{m-n}^{(1)}(k\rho_{l'l})e^{-i(m-n)\phi_{l'l}} \times J_n(k\rho_{li})e^{-in\phi_{li}} \tag{10}$$

Even though $H_{m-n}^{(1)}(x) \to \infty$ when $|m-n| \to \infty$, the above summations converge because $J_n(x) \to 0$, when $|n| \to \infty$. Notice that the inner summation in the above is the convolution of two discrete Fourier series. Therefore, it can be expressed as a product of two functions if their respective discrete Fourier transforms (DFT) can be found. Unfortunately, the DFT of $H_p^{(1)}(x)e^{-ip\phi}$ does not exist since $H_p^{(1)}(x) \to \infty$ when $|p| \to \infty$. However, we can truncate the inner summation since it converges and express eqn. 10 as

$$H_0^{(1)}(k\rho_{ji}) = \sum_{m=-\infty}^{\infty} J_m(k\rho_{jl'})e^{im(\rho_{jl'}-\pi)} \times \sum_{n=m-P}^{m+P} H_{m-n}^{(1)}(k\rho_{l'l})e^{-i(m-n)\phi_{l'l}} \times J_n(k\rho_{li})e^{-in\phi_{li}} \tag{11}$$

Eqn. 11 can be expressed in the Fourier space by using the integral representation of the Bessel function [15, p. 62]

$$J_m(k\rho_{jl'})e^{im\phi_{jl'}} = \frac{1}{2\pi}\int_0^{2\pi} d\alpha e^{ik\rho_{jl'}\cos(\alpha-\phi_{jl'})+im[\alpha-(\pi/2)]} \tag{12a}$$

$$J_n(k\rho_{li})e^{-in\phi_{li}} = \frac{1}{2\pi}\int_0^{2\pi} d\alpha' e^{ik\rho_{ll}\cos(\alpha'+\phi_{li})+in[\alpha'-(\pi/2)]} \quad (12b)$$

Using eqn. 12 in eqn. 11, exchanging the order of integration and summation, we have

$$H_0^{(1)}(k\rho_{ji}) = \frac{1}{2\pi}\int_0^{2\pi} d\alpha \tilde{\beta}_{jl'}(\alpha)\tilde{\alpha}_{l'l}(\alpha)\tilde{\beta}_{li}(\alpha) \quad (13)$$

where

$$\tilde{\alpha}_{l'l}(\alpha) = \sum_{p=-P}^{P} H_p^{(1)}(k\rho_{l'l})e^{-ip[\phi_{l'l}-\alpha-(\pi/2)]} \quad (14)$$

and

$$\tilde{\beta}_{jl'}(\alpha) = e^{ik\rho_{jl'}\cos(\alpha-\phi_{jl'})} \quad \tilde{\beta}_{li}(\alpha) = e^{ik\rho_{li}\cos(\alpha-\phi_{li})} \quad (15)$$

Notice that now, cylindrical waves are replaced by plane waves in the integrand of eqn. 13. Also, $\tilde{\alpha}$ is now replaced by a diagonal operator $\tilde{\alpha}_{l'l}(\alpha)$. Notice now that the series in eqn. 14 diverges if P is increased indefinitely. This results from the exchange of the order of summation and integration.

Using eqn. 13 in replacement of eqn. 5 in eqn. 6, we have

$$\frac{\omega\mu_0}{8\pi}\int_0^{2\pi} d\alpha \tilde{\beta}_{jl'}(\alpha)\sum_{\substack{l=1\\l\neq l'}}^{N/M}\tilde{\alpha}_{l'l}(\alpha)\sum_{i\in G_l}\tilde{\beta}_{li}(\alpha)\Delta_i\alpha_i = b'_j \qquad j\in G_{l'} \quad l'=1,\ldots,N/M \quad (16)$$

for intergroup interactions. The integral in eqn. 13 can be replaced by Q-point summation yielding

$$\frac{\omega\mu_0}{4Q}\sum_{q=1}^{Q}\tilde{\beta}_{jl'}(\alpha_q)\sum_{\substack{l=1\\l\neq l'}}^{N/M}\tilde{\alpha}_{l'l}(\alpha_q)\sum_{i=G_l}\tilde{\beta}_{li}(\alpha_q)\Delta_i a_i = b'_j \qquad j\in G_l \quad (17)$$

Notice that in the above, instead of propagating the field from one group to another using cylindrical waves, one has effectively used plane waves. These plane waves diagonalise the translation operators.

It can be shown that Q above is proportional to M from sampling theorem. With this new equation, the cost of the first step of the calculation, T_1, is still the same. However, the replacement of $\tilde{\alpha}_{l'l}$ with a diagonal operator $\tilde{\alpha}_{l'l}(\alpha_q)$ reduces the cost in the second stage to

$$T_2 = C_1\frac{N^2}{M} \quad (18)$$

The cost in the third stage is still the same. Therefore, the total cost is

$$T = C_1\frac{N^2}{M} + C_2 NM \quad (19)$$

Optimising eqn. 19 with respect to M yields $M = \sqrt{[(C_1/C_2)N]}$. Therefore,

$$T = 2\sqrt{\left(\frac{C_1}{C_2}\right)}N^{1.5} \quad (20)$$

A further nesting of this algorithm within itself yields an $O(N^{4/3})$ algorithm.*

3 Combined field integral equation

A straightforward solution of eqn. 1 is plagued by the problem of internal resonances as the integral operator in eqn. 1 has null spaces at these resonant frequencies. To overcome this, a combined field integral equation [11–13] is used which yields an integral equation with only complex resonant frequencies.

To obtain the combined field integral equation, we multiply both sides of eqn. 1 by a differential operator

$$P(\rho) = 1 + \lambda\hat{n}\cdot\nabla$$

to obtain the combined field integral equation (CFIE)

$$-i\omega\mu_0\int_S P(\rho)g_0(\rho-\rho')J_z(\rho')\,dS' = P(\rho)E_z^{inc}(\rho) \quad (21)$$

where $\hat{n}$ is the unit outward normal at ρ, and λ is a complex constant.

After discretisation, eqn. 21 can be written in a discretised form

$$\sum_{i=1}^{N} G_{ji}a_i = b_j \quad j=1,2,\ldots,N \quad (22a)$$

where

$$G_{ji} = \begin{cases} 30\pi k\Delta_i\left[1 + i\frac{2}{\pi}\ln\left(\frac{\gamma k\Delta_i}{4e}\right) - i\frac{2\lambda}{\Delta_i}\right] & i=j \\ 30\pi k\Delta_i P_j H_0^{(1)}(k\rho_{ji}) & i\neq j \end{cases} \quad (22b)$$

and

$$b_j = P_j E_z^{inc}(\rho_j)$$
$$a_i = J_z(\rho_j)$$
$$P_j = 1 + \lambda\frac{\partial}{\partial n_j} \quad (22c)$$

For H_z polarisation, a similar equation to eqn. 22 can be obtained in a similar manner with $b_j = P_j H_z^{inc}(\rho_j)$, $a_i = H_z(\rho_i)$ and

$$G_{ji} = -\frac{i}{4}\Delta_i P_j\frac{\partial}{\partial n_i}H_0^{(1)}(k\rho_{ji}) \quad i\neq j \quad (23)$$

Using the fact that $(\partial/\partial n_i) = n_x^{(i)}(\partial/\partial x) + n_y^{(i)}(\partial/\partial y)$, where $n_x^{(i)}$ and $n_y^{(i)}$ are the x and y components of the unit normal $\hat{n}_i$, we can show from eqn. 13 that

$$\frac{\partial}{\partial n_i}H_0^{(1)}(k\rho_{ji}) = \frac{1}{2\pi}\int_0^{2\pi} d\alpha\tilde{\beta}_{jl'}(\alpha)\tilde{\alpha}_{l'l}(\alpha)\frac{\partial}{\partial n_i}\tilde{\beta}_{li}(\alpha)$$
$$= \frac{1}{2\pi}\int_0^{2\pi} d\alpha\tilde{\beta}_{jl'}(\alpha)\tilde{\alpha}_{l'l}(\alpha) \times [ik(n_x^{(i)}\cos\alpha + n_y^{(1)}\sin\alpha)]\tilde{\beta}_{li}(\alpha) \quad (24)$$

Using similar idea, we can show that

$$P_j H_0^{(1)}(k\rho_{ji}) = \frac{1}{2\pi}\int_0^{2\pi} d\alpha[1 + i\lambda k(n_x^{(j)}\cos\alpha + n_y^{(j)}\sin\alpha)] \times \tilde{\beta}_{jl'}(\alpha)\tilde{\alpha}_{l'l}(\alpha)\tilde{\beta}_{li}(\alpha) \quad (25)$$

Consequently, eqn. 22 or its variant eqn. 23, after using the discretised form of eqns. 24 or 25, becomes

$$b_j = \sum_{q=1}^{Q}\frac{1}{Q}\tilde{P}_{jl'}(\alpha_q)\sum_{\substack{l=1\\l\neq l'}}^{N/M}\tilde{\alpha}_{l'l}(\alpha_q)\sum_{i\in G_l}\tilde{Q}_{li}(\alpha_q)a_i + \sum_{i\in G_{l'}}G_{ji}a_i \qquad j\in G_{l'} \quad l'=1,\ldots,N/M \quad (26)$$

where

$$\tilde{P}_{jl'}(\alpha_q) = [1 + i\lambda k(n_x^{(j)}\cos\alpha_q + n_y^{(j)}\sin\alpha_q)] \times e^{ik\rho_{jl'}\cos(\alpha_q-\phi_{jl'})} \quad (27)$$

* A reviewer has suggested the possible occurence of relative convergence phenomenon in this algorithm, but we have not observed it.

$$\tilde{Q}_{li}(\alpha_q) = \begin{cases} 30\pi k\Delta_i e^{ik\rho_{li}\cos(\alpha_q - \phi_{li})} & E_z \text{ polarisation} \\ -\dfrac{k\Delta_i}{2}(n_x^{(i)}\cos\alpha_q + n_y^{(i)}\sin\alpha_q)e^{ik\rho_{li}\cos(\alpha_q-\phi_{li})} & H_z \text{ polarisation} \end{cases} \quad (28)$$

The last term in eqn. 26 accounts for interaction within the same group.

4 Dielectric coating hybrid integral equation

Now we shall discuss the application of this algorithm to calculate the scattering solution of dielectric-coated conducting cylinders. Generally, the coating material is modelled by small circular dielectric cylinders as is done by many other authors [18–20]. The equations governing the induced current on the conducting surface will be the same as eqn. 22 except that the contribution from the dielectric region is added to the equations.

When an inhomogeneous dielectric scatterer is closed to a metallic scatterer, the total scattered field from the scatterers for E_z polarisation is

$$E_z^{sca}(\rho) = i\omega\mu_0 \int_S dS' g_0(\rho - \rho')J_z(\rho') + \int_V dV' g_0(\rho - \rho')[k^2(\rho') - k_0^2]E_z(\rho') \quad (29)$$

where $E_z(\rho') = E_z^{inc}(\rho') + E_z^{sca}(\rho')$. The boundary condition on the metallic surface is $E_z^{sca}(\rho') = -E_z^{inc}(\rho')$. The dielectric region can be replaced by circular dielectric subscatterers [18–20]. Hence, the second part of eqn. 29 can be discretised and expressed as

$$E_z^{sca}(\rho) = i\omega\mu_0 \int_s dS' g_0(\rho - \rho')J_z(\rho') + \sum_{i=N+1}^{N'} \psi_0(\rho_i)a_i \quad (30)$$

This is because each dielectric subscatterer scatters like a monopole for E_z polarisation. If the isolated T-matrix of each dielectric subscatterer is known, then the constraint condition on each dielectric subscatterer is that [15, 18]

$$a_j = T_{j(1)}E_z(\rho_j) \quad j = N+1, \ldots, N' \quad (31)$$

Therefore, discretising the first part of eqn. 30 as well as before, and imposing the boundary condition on the metallic surface analogous to eqn. 3, we have

$$\sum_{i=1}^{N} g_{ji}a_i - \sum_{i=N+1}^{N'} \psi_0(\rho_{ji})a_i = b_j \quad j = 1, .., N \quad (32)$$

Imposing eqn. 31 on the dielectric subscatterers, we have

$$a_j = T_{j(1)}\left\{E_z^{inc}(\rho_j) - \sum_{i=1}^{N} g_{ji}a_i + \sum_{i=N+1}^{N'} \psi_0(\rho_{ji})a_i\right\} \quad j = N+1, \ldots, N' \quad (33)$$

Eqns. 32 and 33 constitute N' equations for the N' unknowns a_i, $i = 1, \ldots, N'$. However, it is still plagued with internal resonances from the metallic scatterer. To overcome this, eqn. 30 is operated upon by the $P(\rho)$ operator before the boundary condition is imposed on the metallic surface. By so doing, we convert eqn. 32 to

$$\sum_{i=1}^{N} G_{ji}a_i - \sum_{i=N+1}^{N'} P_j\psi_0(\rho_{ji})a_i = b_j \quad j = 1, \ldots, N \quad (34)$$

analogous to eqn. 22*a*. Eqns. 33 and 34 constitute the equations free of internal resonance problem. The fast multipole method can be used to speed up the matrix–vector multiplication as before, if the dielectric region is a thin coating on the metallic scatterer.

Similar equations can be derived for H_z polarisation. In this case, the expression for the scattered field looks like

$$H_z^{sca}(\rho) = \int_S dS' \frac{\partial g_0(\rho - \rho')}{\partial n'} H_z(\rho') + \int_V dV \nabla g_0(\rho - \rho')[\varepsilon_r^{-1}(\rho') - 1]\nabla H_z(\rho') \quad (35)$$

For this polarisation, the scattered field of a small dielectric cylinder is $\boldsymbol{\psi}^t(\rho)\cdot\boldsymbol{a}$, where $\boldsymbol{a}$ contains the harmonics coefficient to represent a dipole scattered field. It is related to incident wave $\phi^{inc} = \boldsymbol{\psi}^t(\rho)\cdot\boldsymbol{a}_0$ by the isolated $\boldsymbol{T}$-matrix [15–18] such that

$$\boldsymbol{a} = \bar{\boldsymbol{T}}_{(1)}\cdot\boldsymbol{a}_0 \quad (36)$$

Discretising the integral equation as before and using the idea of combined field integral equation, we can form the equations for coated-conductor cylinders as

$$\sum_{i=1}^{N} G_{ji}a_i + \sum_{i=N+1}^{N'} P_j\boldsymbol{\psi}^t(\rho_{ji})\cdot\boldsymbol{a}_i = b_j \quad j = 1, 2, \ldots, N \quad (37a)$$

$$\boldsymbol{a}_j = \bar{\boldsymbol{T}}_{j(1)}\cdot\left\{\bar{\boldsymbol{\beta}}_{j0}\boldsymbol{a}_0 + \sum_{i=1}^{N}\bar{\boldsymbol{\alpha}}_{ji}\cdot\boldsymbol{p}_i a_i + \sum_{i=N+1, i\neq j}^{N'}\bar{\boldsymbol{\alpha}}_{ji}\cdot\boldsymbol{a}_i\right\} \quad j = N+1, N+2, \ldots, N' \quad (37b)$$

where $\boldsymbol{p}_i$ is the polarisation vector $\boldsymbol{p}_i^t = [kn_i/2, 0, kn_i^*/2]$.

5 Numerical results

To verify the algorithm, the RCS of a conducting circular cylinder is calculated for different radius (R) and compared with exact solutions (closed form solution).

Fig. 2A shows the RCS of an E_z-polarised wave at 0° incidence of a circular cylinder with radius $R = 1.9658\lambda_0$

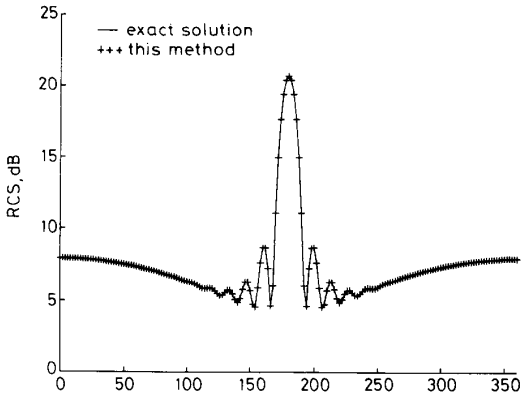

Fig. 2A *RCS of an E_z-polarised wave at 0° incidence of a circular conducting cylinder with radius $R = 1.9658\lambda_0$ where internal resonance occurs*

(for this cylinder, internal resonances occur at $R = 1.9658\lambda_0$ and $R = 2.0714\lambda_0$). Fig. 2B shows the current distribution derived by this method using the combined field integral equation (CFIE) after nine iterations, and this method using the electric field integral equation (EFIE) after 83 iterations. The smooth current distribution of this method with the CFIE shows that the result is not affected by internal resonances, whereas if the

EFIE is used with this method, the error is quite large even after 83 iterations. A similar result is obtained for the $R = 2.0714\lambda_0$ case.

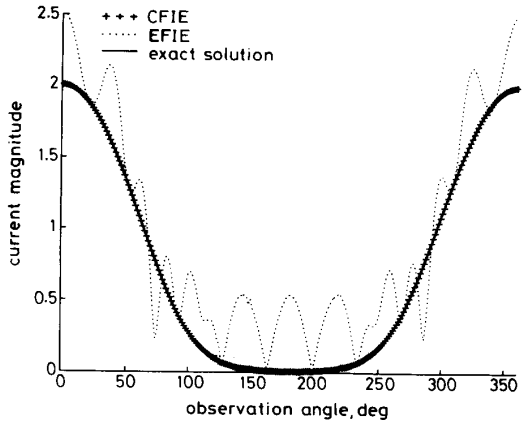

Fig. 2B *Comparison of the current distributions for the case in Fig. 2A using this method with the combined field integral equation (CFIE), electric field integral equation (EFIE) and exact solution*

Fig. 3 shows the RCS for $R = 50\lambda_0$. In this Figure, because of the fast oscillation, only a small portion in the forward direction is plotted. It is seen that the agreement with the closed-form solution is excellent both for scattered field and induced current distribution.

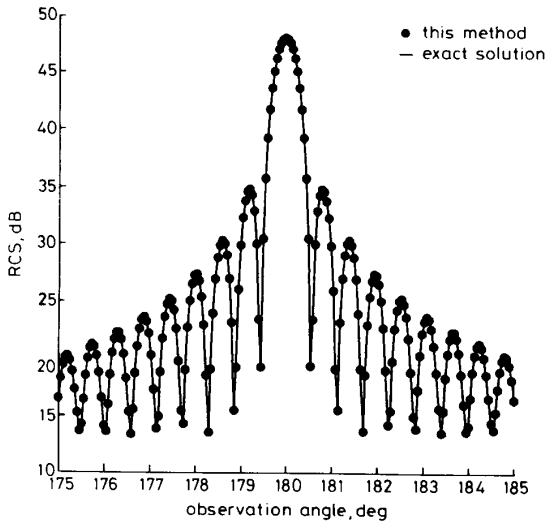

Fig. 3 *RCS for a circular conducting cylinder with $R = 50\lambda_0$*

In Fig. 4, the increase of CPU time with unknowns N is plotted on a log–log scale. We find that the slope of the curve is approximately 1.5, showing the relationship CPU time $\propto N^{1.5}$.

Fig. 5A shows the RCS for a dielectric-coated circular conducting cylinder for E_z-polarised incident waves. Fig. 5B similarly shows that for H_z-polarised incident waves. The radius of the circular cylinder is $2\lambda_0$ and the thickness of the coating is $0.047\lambda_0$, with $\varepsilon_r = 2 + i0.2$ and $\mu_r = 1.4 + i0.672$. The frequency is 300 MHz. From the Figure we can see that, even for lossy material coating, the computed result and the closed-form solution agree well.

Fig. 6 shows the RCS for a dielectric-coated ogive calculated using this method and RATMA (recursive aggregate T matrix algorithm) [21] for E_z polarisation. The results are in excellent agreement. The ogive is made from two arcs with radius of curvature of $3\lambda_0$. The height of the ogive is $1\lambda_0$ while the thickness of the dielectric

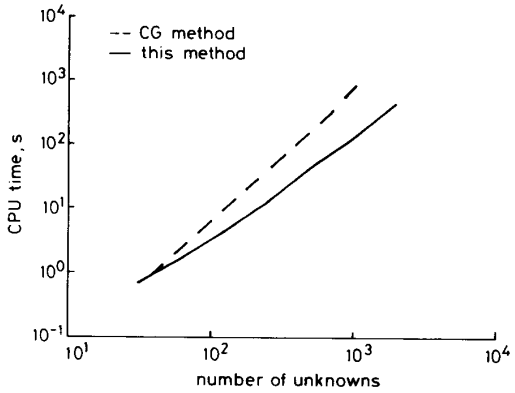

Fig. 4 *Increase of CPU time with unknowns N plotted on a log–log scale*

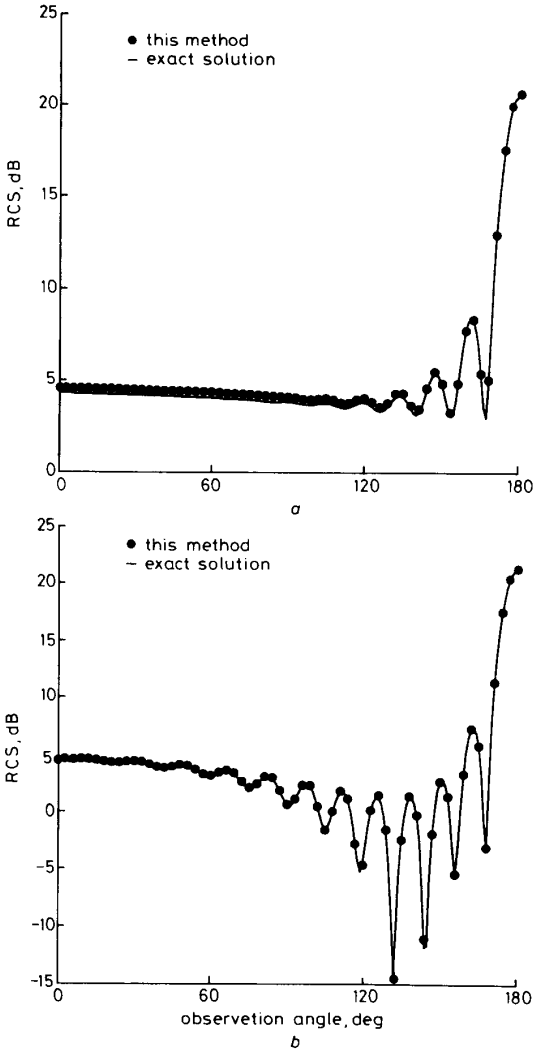

Fig. 5 *RCS for dielecric-coated circular conducting cylinder. Radius of the circular cylinder is $2\lambda_0$ and the thickness of the coating is $0.047\lambda_0$, with $\varepsilon_r = 2 + i0.2$ and $\mu_r = 1.4 + i0.672$. The frequency is 300 MHz*

a E_z-polarised incident waves
b H_z-polarised incident waves

coating is $0.049\lambda_0$. The incident wave is at 90°, normal to the long axis of the ogive. The dielectric coating has $\varepsilon_r = 2 + i0.2$ and $\mu_r = 1$.

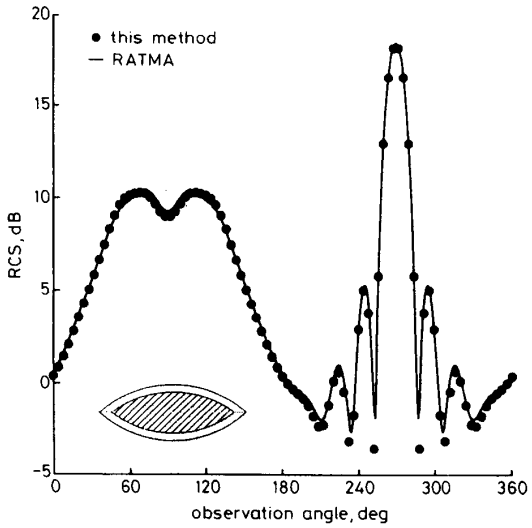

Fig. 6 *RCS for a dielectric-coated ogive calculated using this method and RATMA (recursive aggregate T matrix algorithm) for E_z polarisation*

6 Conclusion

A fast algorithm is developed for the scattering calculation of conducting cylinders for both H_z and E_z polarisation. Internal resonance problem is removed by using a combined field integral equation. We also extend the algorithm for dielectric-coated conducting cylinders using a hybrid of a combined field surface integral equation and a volume integral equation. Provided that the coating is thin (typically less that 0.1 wavelength), the fast multipole method is used to accelerate the speed of the solution. The computed result for a different size cylinder is in good agreement with the exact series solution. The speed of the algorithm is much faster than both the N^3 and N^2 algorithm. Hence, it can be applied to much larger objects.

7 References

1 WEI, K., and VAN BLADEL, J.: 'Low frequency scattering by rectangular cylinders', *IEEE Trans.*, 1963, **AP-11**, pp. 52–56

2 WILTON, D.R., and MITTRA, R.: 'A new numerical approach to the calculation of electromagnetic scattering properties of two-dimensional bodies of arbitrary cross section', *IEEE Trans.*, 1972, **AP-20**, pp. 310–317

3 ARVAS, E., RAO, S.M., and SARKAR, T.K.: 'E-field solution of TM-scattering from multiple perfectly conducting and lossy dielectric cylinders of arbitrary cross section', *IEE Proc. H*, 1986, **133**, pp. 322–324

4 RICOY, M.A., KILBERG, S.L., and VOLAKIS, J.L.: 'Simple integral equation for two-dimensional scattering with further reduction in unknowns', *IEE Proc. H*, 1989, **136**, (4), pp. 298–304

5 UMASHANKAR, K., CHUN, W., and TAFLOVE, A.: 'A simple analytical solution to electromagnetic scattering by two-dimensional conducting objects with edges and corners, Part I: TM polarization', *IEEE Trans.*, 1991, **AP-39**, (9), pp. 1332–1337

6 KISHK, A.A., GLISSON, A.W., and GOGGAN, D.M.: 'Scattering form conductors coated with materials of arbitrary thickness', *IEEE Trans.*, 1992, **AP-40**, (1), pp. 108–111

7 HARRINGTON, R.F.: 'Field computation by moment methods' (Krieger, Marlabar, Florida, 1982), p. 41

8 PRESS, W.H., FLANNERY, B.P., TEUKOLSKY, S.A., and VETTERING, W.T.: 'Numerical Recipes' (Cambridge University Press, 1989), p. 301

9 ROKHLIN, V.: 'Rapid solution of integral equations of scattering theory in two dimensions', *J. Comput. Phys.*, 1990, **86**, (2), pp. 414–439

10 ENGHETA, N., MURPHY, W.D., ROKHLIN, V., and VASSILIOU, M.S.: 'The fast multipole method (FMM) for electromagnetic scattering problems', *IEEE Trans.*, 1992, **AP-40**, (6), pp. 634–641

11 WERNER, P.: 'On the exterior boundary value problem of perfect reflection for stationary electromagnetic waves', *J. Math. Anal. Appl.*, 1963, (7), pp. 348–396

12 PANICH, O.I.: 'On the Question of the solvability of the exterior boundary-value problems for the wave equation and Maxwell's equation', *Russian Math. Surveys*, 1965, **20**, pp. 221–226

13 MITZNER, K.M.: 'Numerical solution of the exterior scattering problem at the eigenfrequencies of the interior problem', *URSI Meeting Digest*, 1968, p. 76

14 CHEW, W.C.: 'An N^2 algorithm for the multiple scattering solution of N scatterers', *Microw. Opt. Technol. Lett.*, 1989, **2**, (1), pp. 380–383

15 CHEW, W.C.: 'Waves and fields in inhomogeneous media' (Van Nostrand Reinhold, New York, 1990)

16 WANG, Y.M., and CHEW, W.C.: 'An efficient algorithm for solution of a scattering problem', *Microw. Opt. Technol. Lett.*, 1990, **3**, (3), pp. 102–106

17 CHEW, W.C., and WANG, Y.M.: 'A fast algorithm for solution of a scattering problem using a recursive aggregate tare matrix method', *Microw. Opt. Technol. Lett.*, 1990, **3**, (5), pp. 164–169

18 CHEW, W.C., GUREL, L., WANG, Y.M., OTTO, G., WAGNER, R., and LIU, Q.H.: 'A generalized recursive algorithm for wave-scattering solutions in two dimensions', *IEEE Trans.*, 1992, **MTT-40**, (4), pp. 716–723

19 RICHMOND, J.H.: 'Scattering by a dielectric cylinder of arbitrary cross section shape', *IEEE Trans.*, 1965, **AP-13**, pp. 334–341

20 RICHMOND, J.H.: 'TM scattering by a dielectric cylinder of arbitrary cross section shape', *IEEE Trans.*, 1966, **AP-14**, pp. 460–464

21 LIN, J.H., and CHEW, W.C.: 'Solution of oblong, dielectric coated, metallic scatterer by the recursive algorithm', *Electron. Lett.*, 1992, **28**, (2), pp. 185–186